Biomaterials 35 (2014) 9012–9022

Contents lists available at ScienceDirect

Biomaterials

journal homepage: www.elsevier.com/locate/biomaterials

Intravascular cell delivery device for therapeutic VEGF-induced angiogenesis in chronic vascular occlusion

Arun H.S. Kumar [a, 1], Kenneth Martin [a, 1], Brendan Doyle [b], Chien-Ling Huang [a], Gopala-Krishnan M. Pillai [a], Mohammed T. Ali [a], Kimberly A. Skelding [b], Shaohua Wang [b], Birgitta M. Gleeson [a], Saleem Jahangeer [c], Erik L. Ritman [d], Stephen J. Russell [e], Noel M. Caplice [a, b, *]

[a] Centre for Research in Vascular Biology (CRVB), Biosciences Institute, University College Cork, Cork, Ireland
[b] Division of Cardiovascular Diseases, Molecular Medicine Program, Mayo Clinic, Rochester, MN, USA
[c] Cork Cancer Research Centre, Biosciences Institute, University College Cork, Cork, Ireland
[d] Department of Physiology and Biomedical Engineering, Mayo Clinic, Rochester, MN, USA
[e] Division of Hematology, Molecular Medicine Program, Mayo Clinic, Rochester, MN, USA

ARTICLE INFO

Article history:
Received 16 May 2014
Accepted 10 July 2014
Available online 2 August 2014

Keywords:
Angiogenesis
Gene therapy
Intravascular stent
Smooth muscle cells
Blood flow

ABSTRACT

Site specific targeting remains elusive for gene and stem cell therapies in the cardiovascular field. One promising option involves use of devices that deliver larger and more sustained cell/gene payloads to specific disease sites using the versatility of percutaneous vascular access technology. Smooth muscle cells (SMCs) engineered to deliver high local concentrations of an angiogenic molecule (VEGF) were placed in an intravascular cell delivery device (ICDD) in a porcine model of chronic total occlusion (CTO) involving ameroid placement on the proximal left circumflex (LCx) artery. Implanted SMC were retained within the ICDD and were competent for VEGF production *in vitro* and *in vivo*. Following implantation, micro-CT analyses revealed that ICDD-VEGF significantly enhanced vasa vasora microvessel density with a concomitant increase in tissue VEGF protein levels and formation of endothelial cell colonies suggesting increased angiogenic potential. ICDD-VEGF markedly enhanced regional blood flow determined by microsphere and contrast CT analysis translating to a functional improvement in regional wall motion and global left ventricular (LV) systolic and diastolic function. Our data indicate robust, clinically relevant angiogenesis can be achieved in a human scale porcine chronic vascular occlusion model following ICDD-VEGF-based delivery of angiogenic cells. This may have implications for percutaneous delivery of numerous therapeutic factors promoting creation of microvascular bypass networks in chronic vaso-occlusive diseases.

1. Introduction

Chronic vaso-occlusive disease remains the Achilles heel of cardiovascular medicine and surgery [1]. Percutaneous revascularization of chronic occlusion is hampered by the risk of arterial perforation, reduced primary success and high restenosis rates [2]. Moreover, conventional surgical strategies aimed at bypassing these occlusive lesions are frequently not feasible because of the poor condition of distal blood vessels [3] or co-morbidities in the target population [4]. The need for alternative revascularization strategies is great and for more than two decades, gene and cell therapy have offered tantalizing prospects for alleviation of such no-option occlusive vasculopathies. However, despite initial promise, significant barriers have emerged to both vector delivery and exogenous cell retention at the site of vascular disease [5].

* Corresponding author. Rm. 2.40, CRVB, Biosciences Institute, University College Cork, Cork, Ireland. Tel.: +353 21 490 1329.
E-mail address: n.caplice@ucc.ie (N.M. Caplice).
[1] These are co-first authors of the manuscript.

http://dx.doi.org/10.1016/j.biomaterials.2014.07.016

Previous animal studies employing local VEGF-based gene therapy strategies have been limited by the amount and duration of gene delivery that can be achieved in the vessel wall [6] as well as safety concerns including angioma formation [7]. To achieve sustained delivery at a safe local dose, we adopted a strategy of placing therapeutic cells, engineered with an angiogenic gene, into a percutaneously deliverable intravascular cell delivery device (ICDD) incorporating a non-woven matrix that allowed a 3D cell mass to be stably conditioned in culture (Fig. 1). The approach of utilizing an expanded autologous cell source as an angiogenic gene/protein delivery platform is considered to obviate some of the reliability, dosing and technical challenges associated with direct *in vivo* viral vector administration [8]. We hypothesized that such an ICDD would elicit a more robust, stable and reliable local biologic response than cells or genes alone and that this would facilitate targeted, sustained and therapeutic angiogenesis in the myocardium supplied by the occlusive artery.

We selected autologous SMCs as a conduit for VEGF delivery and expression for several reasons: 1) we hypothesized that these cells would be a more stable source for gene transfer than vector alone 2) in previous experiments, we had shown that SMC could be delivered on a stent-based platform in 100-fold greater numbers than endothelial cells [9]. 3) SMC grow in multilayers within the mesh allowing development of a stable organoid that does not embolize 4) autologous SMC are also a clinically translatable cell as they can

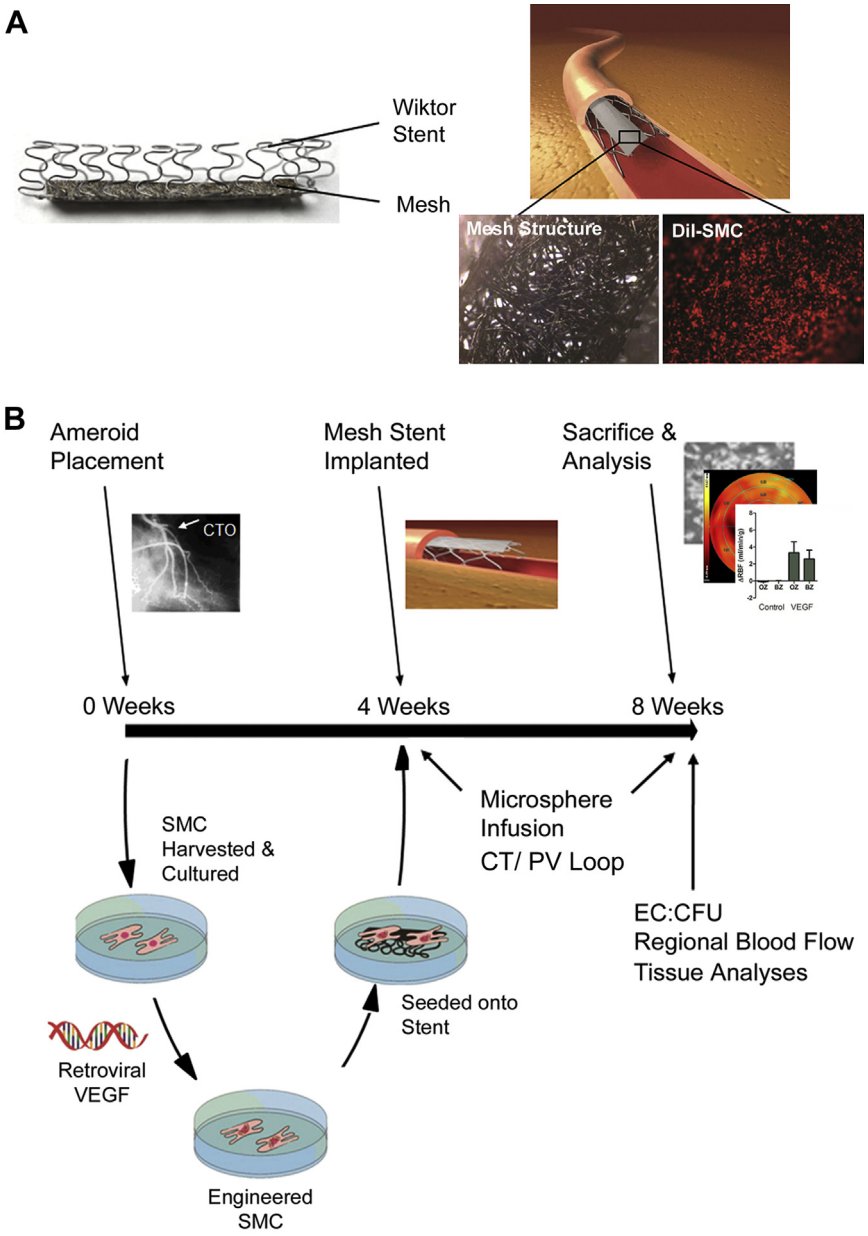

Fig. 1. Overview of ICDD strategy and chronic total occlusion (CTO) study protocol. A. SMC within ICDD Inset showing non-woven mesh topography with the ability to accomodate adherent DiI-labeled SMC. **B**. CTO was induced by ameroid constrictor placement on the proximal LCx. SMCs simultaneously harvested from the jugular vein were transduced with a retroviral VEGF expression vector and loaded onto an ICDD prior to deployment four weeks after ameroid placement. CT, microsphere and conductance catheter analyses were performed at the time of ICDD-VEGF placement and one month later (sacrifice) along with further tissue analyses.

be isolated from autologous superficial vein digestion or from peripheral blood progenitors in substantial numbers and 5) SMC secrete complementary growth factors such as PDGF in addition to $VEGF_{165}$ which might encourage local arteriogenesis rather than capillary-like angiogenesis seen with previous single VEGF gene therapy [10]. Previously, cell viability and local stability of GFP reporter-labeled SMC at 30 days in the normal artery was established using this platform [9]. We thus engineered an ICDD to provide stable SMC-based VEGF delivery *in vivo*. In the current study, therapeutic efficacy of this cell/gene delivery system was structurally and functionally assessed in terms of improvement in myocardial blood flow (MBF) and global left ventricular function in a porcine model of chronic ischemia. Additionally, ischemic zone arteriogenesis and circulating progenitor cell responses were investigated. Development of this ICDD platform may have implications for gene and cell therapy treatment of numerous cardiovascular disease processes including cardiac and peripheral ischemia.

2. Materials & methods

2.1. ICDD preparation, smooth muscle cell harvest, transduction and seeding

Our delivery strategy involved genetically engineered and non-transduced control SMC seeded in a non-woven metallic matrix fixed on a conventional stent (Fig. 1(A)) and was prepared as previously described [9]. Briefly, a 5 mm × 20 mm mesh was made from a fiber matrix produced by compressing metallic fibers (Bekaert Fibre Technologies, Marietta, GA) into a felt and then sintering the matrix. This was attached to a fully expanded 20 mm stent and sealed with a gas tungsten arc welding torch. The ICDD was cleaned by sonication several times in absolute ethyl alcohol, washing in Haemo-Sol (4.5 g/250 ml of water) for 30 min of rocking, rinsing several times in filtered sterile water, washing in absolute alcohol, and gas sterilized. The ICDD was coated with 10 μg/ml fibronectin (Sigma) prior to cell seeding. Animals were subsequently randomized to receive either Control or VEGF-secreting ICDD. Autologous porcine smooth muscle cells were obtained from a 2–3 cm segment of external jugular vein obtained at the initial surgical encounter. Cells were dispersed from the intima and media of the vessel through a series of collagenase and elastase digestions [11]. SMCs at culture passage 1–2 were transduced with retroviral VEGF vector at 100 MOI, followed by puromycin (10 μg/ml, Sigma) selection. Medium was changed to M199 (serum free, Sigma), and conditioned medium was collected after 24 h replacement. ELISA (Abcam) and immunoflouresence (rabbit anti-human VEGF, Santa Cruz) was used to confirm VEGF production. Confirmation of smooth muscle cell identity was made through positive α-smooth muscle actin, calponin and smooth muscle myosin heavy chain and lack of von Willebrand factor staining, control or VEGF-secreting were seeded on the mesh backbone of the ICDD at a density of 1.0×10^7 cells/cm^2. ICDD-Control devices were seeded at the same density with non-engineered SMC.

2.2. Chronic total vascular occlusion porcine model

All animal protocols were approved by the Institutional Animal Use and Care Committee at the Mayo Clinic, Rochester, USA and University College Cork, Cork, Ireland and were in accord with the National Institutes of Health guide for the care and use of laboratory animals. Thirty seven domestic female Yorkshire/Landrace pigs (22–27 kg) were used in this study (10 for ICDD implantation without CTO, 11 for regional blood flow (RBF) analysis with CTO, 16 for functional studies with CTO, four deaths overall). Pigs were initially anesthetized with xylazine (1.6 mg/kg), telazol (3.3 mg/kg) and glycopyrolate (0.14 mg/kg) in a weight adjusted manner maintained using inhalational isofluorane 1.5%. Using sterile technique, a 2.5 mm ameroid constrictor was placed *via* a left thoracotomy on the left circumflex artery allowing sufficient space for later stent deployment [12]. During this procedure the external jugular vein was also obtained for smooth muscle cell harvest. After recovery the animals remained in colony housing for 4 weeks. Surgical wounds were closed using 6/0 suture and sealed with Aluspray aerosol bandage (Neogen). Gentamycin: 4 mg/kg s.c. was administered as a single dose during the course of the ameroid placement procedure and Piperacillin-Tazobactum (4 g/0.5 g respectively) was additionally administered daily for first five days post-procedure. Analgesia was delivered as s.c. administration of carprofen (2 mg/kg) every 24 h for three days following the procedures. Following the initial phase of procedure optimization, a mortality rate of ~10% which occurred in the early peri- and post-operative phases was observed. All animals that died were excluded from analysis. There was no difference in mortality between treatment groups.

2.3. ICDD deployment and coronary angiography

At 4 weeks following ameroid placement, occlusion was verified by coronary angiography and collateral formation was assessed (Fig. 1(B)) and animals with collaterals were excluded from further study. Immediately following diagnostic angiography balloon size was selected based on angiographic appearance (2.5–3.5 mm) and the ICDD crimped using a mechanical crimping device and then balloon mounted. Deployment was performed using a 8F JL3.5 mm guiding catheter and *via* a guidewire through a sheath placed *via* cut-down of the external carotid artery and under direct angiographic guidance. One to two low pressure inflations were performed to deploy the ICDD as close as possible to the site of ameroid placement. All animals were pretreated for 48 h with aspirin (4 mg/kg), clopidigrel (0.9 mg/kg) and verapamil (1.5 mg/kg). Aspirin and clopidigrel were continued until sacrifice date. Prior to sacrifice (4 weeks after stent placement), repeat angiography was performed to evaluate collateral formation. Hemodynamic and electrocardiographic monitoring was performed for all invasive procedures. Animal sacrifice was performed under anesthesia utilizing an intravenous sodium pentobarbital injection.

2.4. Tissue processing, histological and immunofluorescent staining analyses

For all analyses, operators were blinded as to the group from which the samples originated. At sacrifice, the heart was immediately harvested and samples were obtained. Sections of myocardial areas of interest supplied by the left circumflex artery were obtained adjacent to ameroid placement and were directly placed in OCT medium (CellPath). The ICDD was removed by dissection of a small section of myocardium immediately overlying the vessel wall and plastic embedded for sectioning as described previously [13]. The ameroid constrictor was visualized to verify the degree of occlusion. The remaining myocardium including the region supplied by the CTO/ICDD was placed in 4% formalin for fixation. Microvessels were identified and quantified using immunofluorescent staining of α-SMA (clone 1A4, Dako) and CD31 (rabbit polyclonal, Abcam) followed by imaging using confocal microscopy (Nikon eC1 plus, TE2000E).

2.5. Endothelial colony identification

At baseline, prior to ameroid placement, at time of ICDD deployment and prior to sacrifice, 50 ml samples of whole blood were obtained for analysis. Using a Ficoll density gradient, the mononuclear cell layer was obtained and was cultured on a fibronectin coated 12 well plates with endothelial differentiation medium EGM-2 as previously described [14]. Culture media was changed at 3, 6 and 9 days at which time colony counting was performed. Endothelial cell colonies were initially identified morphologically using light microscopy and verification was made using endothelial marker staining.

2.6. Micro-CT imaging and analysis

Coronary arteries implanted with ICDD-Control or ICDD-VEGF were prepared and scanned using micro-CT as previously described [15]. Briefly arteries were scanned in 2 cm contiguous segments along the length of the vessel 2 cm either side of the implanted region and within the device segment along the luminal axis. The micro-CT scanner was configured so that the cubic voxel dimension was 20 μm (16 bit gray scale). Three dimensional images were displayed using image analysis software (Analyze 4.0, Biomedical Imaging resource, Mayo Clinic, Rochester, MN). In each cross section vasa vasorum were manually identified and vasa vasorum spatial density (number of vasa vasorum/mm^2 vessel wall area) assessed across each stented segment. The mean value for multiple slices per 2 cm coronary segment was derived for each animal.

2.7. Microsphere injection and processing

Colored fluorescent microspheres were injected into the left ventricle through a pigtail catheter at 4 weeks following ameroid placement and 4 weeks following stent implantation. Injections of 5.0×10^6 microspheres were performed during a resting conditions as well as adenosine administration (400 μg/kg/min)-mediated maximal vasodilatation [16] as described previously [17]. Withdrawal of reference samples was performed through a 7F guiding catheter placed in the descending thoracic aorta through a sheath placed *via* a femoral artery cut-down procedure at a rate of 8 ml/min using a Harvard pump. After formalin fixation, the myocardium was divided into 3 short axis sections (apex, mid, base). These sections were then further divided into circumferential wedge sections of epicardial and endocardial tissue (<3 g). This tissue was weighed and sent for automated fluorescence counting (Interactive Medical Technologies, Irvine CA). RBF measurements were made using the formula: RBF (ml/min/gram) = (total tissue microspheres)/(tissue weight,g)*(reference spheres/ml/min). The change in RBF between and, ΔRBF was calculated by subtracting the RBF at stenting from the RBF value at sacrifice for each sample.

2.8. Tube formation and SMC-EC association assays

Tube formation for *in vitro* angiogenesis analysis was performed as previously described [18]. Briefly, a 96-well plate was coated with 50 μl of Matrigel (Becton Dickinson Labware, Bedford, MA), which was allowed to solidify at 37 °C for 1 h. Human endothelial cells (1.5×10^4 cells per well) labeled with CellTracker Green (Molecular Probes) were treated with conditioned media from control or VEGF-secreting SMC, co-seeded with smooth muscle cells (1.5×10^3 cells per well) labeled with CellTracker Orange on the Matrigel and cultured in M199 conditioned medium, respectively. The cells were incubated for 20 h, and complete tubes from randomly chosen fields were captured using Nikon EZC1-3.30 software on a confocal microscope system (Nikon eC1 plus, TE2000E). Tube length, network area and SMC-EC coverage analysis were performed using ImageJ software (NIH, Bethesda, MD).

2.9. Sixty-four-slice CT imaging, image reconstruction and data analysis

Cardiac CT imaging was performed using a 64-slice scanner (GE Discovery VCT RX) with Iodixanol (Visipaque 320; Amersham Health) contrast agent. All gated CT images were reconstructed at a 1.25 mm slice thickness, and phase data on all axial slices were reconstructed from 0% to 99% of the cardiac cycle in 9% increments for assessment of LV function parameters and ejection fraction (EF), as calculated on an online workstation (AW 4.4; GE Healthcare). Sixty-four-slice images were analyzed with CardIQ software (AW 4.4) to generate polar maps of regional wall motion and quantified as mm^2/g myocardial mass/cardiac cycle. Myocardial perfusion was evaluated by contrast intensity 5 s after bolus injection as described previously [17]. Relative Hounsfield Unit (HU) measurement was calculated as the mean HU in the LC*x*-related region compared to mean HU in the LV chamber and normalized to the initial scan at the time of ameroid constrictor placement.

2.10. Statistical analyses

For *in vivo* experiments, significance was calculated using the Kruskal Wallis test followed by Dunn's Multiple Comparison test. For *in vitro* analyses, comparisons between treatment groups were made using ANOVA and Mann Whitney tests.

3. Results

3.1. ICDD-VEGF and local angiogenic indices in vivo

Seeding densities of approximately 1×10^7 SMC per cm^2 of ICDD were achieved *in vitro* over a 7 day period (Fig. 2(A) and Supplementary Fig. I). Immunofluorescence analyses display the expected staining pattern for the VEGF165 isoform which is both secreted from the Golgi apparatus and identified as bound in extracellular matrix [19] in a punctuate granular localization pattern (Fig. 2(A)). VEGF secretion from the cell mass within the ICDD was confirmed by ELISA to be in the nanogram/ml range (Fig. 2(B)). There was no observable difference in growth rate between untransduced and VEGF-producing SMCs. To examine *in vivo* cell retention, autologous SMC were seeded into an ICDD and implanted into normal porcine coronary arteries. Retention of the cell mass was confirmed using green fluorescent protein (GFP) tracking, within the recipient vessel at 4 weeks after implantation with no evidence of implanted cell migration outside of mesh or into the perivascular space (Fig. 2(C)). Local angiogenic potential of ICDD-VEGF was evaluated using micro-CT (Fig. 2(D)) and compared to untransduced SMC within ICDD-Control groups [20]. ICDD-VEGF induced $a > 2$ fold augmentation in vasa vasorum density within an arborized vascular network extending across internal and external vasa vasorum ($p < 0.01$, Fig. 2(E)). Secreted VEGF in the region of the ICDD-VEGF was quantified by ELISA analysis of tissue within and outside of the ICDD-VEGF recipient coronary artery segments. Local VEGF concentrations were increased >10 fold within the recipient vessel segments compared to the surrounding region or ICDD-Control treated animals (Fig. 2(F)). These data underscore marked accumulation of VEGF within a restricted region of the ICDD-VEGF recipient artery and a gradient of VEGF to the surrounding tissue. As high local VEGF concentrations have previously been intimately linked to endothelial progenitor cell (EPC, Supplementary Fig. II) mobilization [21], we tested, by endothelial cell colony forming unit (EC:CFU) assay (Fig. 2(G)), vasculogenic potential of peripheral blood mononuclear cells obtained from ICDD-VEGF and ICDD-Control-treated animals. $a > 5$ fold increase in EC:CFU in culture was observed in ICDD-VEGF animals compared to controls (Fig. 2(H)).

3.2. ICDD-VEGF placement and regional MBF

Myocardial perfusion, evaluated by contrast multi-detector computed tomography (MD–CT) [17], confirmed enhanced perfusion in ventricular wall supplied by ischemic LC*x* in ICDD-VEGF but not in ICDD-Control (Fig. 3(A and B)). Moreover, real time angio-fluoroscopy indicated, in some animals with ICDD-VEGF, the presence of bridge collateral formation across the occlusive segment with anterograde perfusion of the distal artery (Supplementary video). Regional MBF was evaluated using gold standard colored microsphere analysis. Previous studies have evaluated perfusion in healthy porcine myocardium as between 0.8 and 1.0 ml/min/gramme of tissue [22]. Our baseline data was consistent with these values (Supplementary Fig. VI). At baseline, under resting conditions, treated animals with ICDD-VEGF had a ~20 fold increase in MBF within the occlusive and border zones of the ischemic myocardium (Fig. 3(C)). This increased blood flow was observed in both the endocardial and epicardial ischemic compartments across the full length of the left ventricular chamber (base, midzone, apex). Animals with ICDD-VEGF exhibited a 3–5 fold increase in MBF during adenosine stress in both the occlusive and border zones respectively compared to controls. These increased stress perfusion effects were evident across all ischemic myocardial segments from ventricular base to apex (Fig. 4).

Supplementary video related to this article can be found at http://dx.doi.org/10.1016/j.biomaterials.2014.07.016.

3.3. VEGF-secreting cells and angiogenesis

Analysis of angiogenesis in the myocardium distal to the site of occlusion by immunofluoresence revealed increased numbers of α-smooth muscle actin and CD31 dual positive arterioles (Fig. 5(A)) in ICDD-VEGF when compared to ICDD-Control animals ($p < 0.001$, Fig. 5(B)). To examine the arteriogenic capacity of VEGF-producing SMC in a defined system, conditioned media driven EC and EC/SMC tube formation in matrigel were performed. Conditioned media from VEGF-secreting but not control SMC significantly enhanced EC tube network formation in terms of network area ($p < 0.05$, Fig. 5(C and D)) and perivascular SMC integration into these EC networks ($p < 0.05$, Fig. 5(E and F)).

3.4. ICDD-VEGF and LV function following CTO

Whether the improvements elicited by ICDD-VEGF placement in regional blood flow translated to improvements in hemodynamic function was evaluated since the extent of myocardial injury and LV function may be correlated with the degree of therapeutic arteriogenesis in patients with CTO [23]. Global and regional LV function and hemodynamics were assessed four weeks after ICDD placement using cardiac CT and conductance catheter measurements. ICDD-VEGF significantly improved global LV ejection fraction by CT (Fig. 6(A)), dp/dt by PV loop

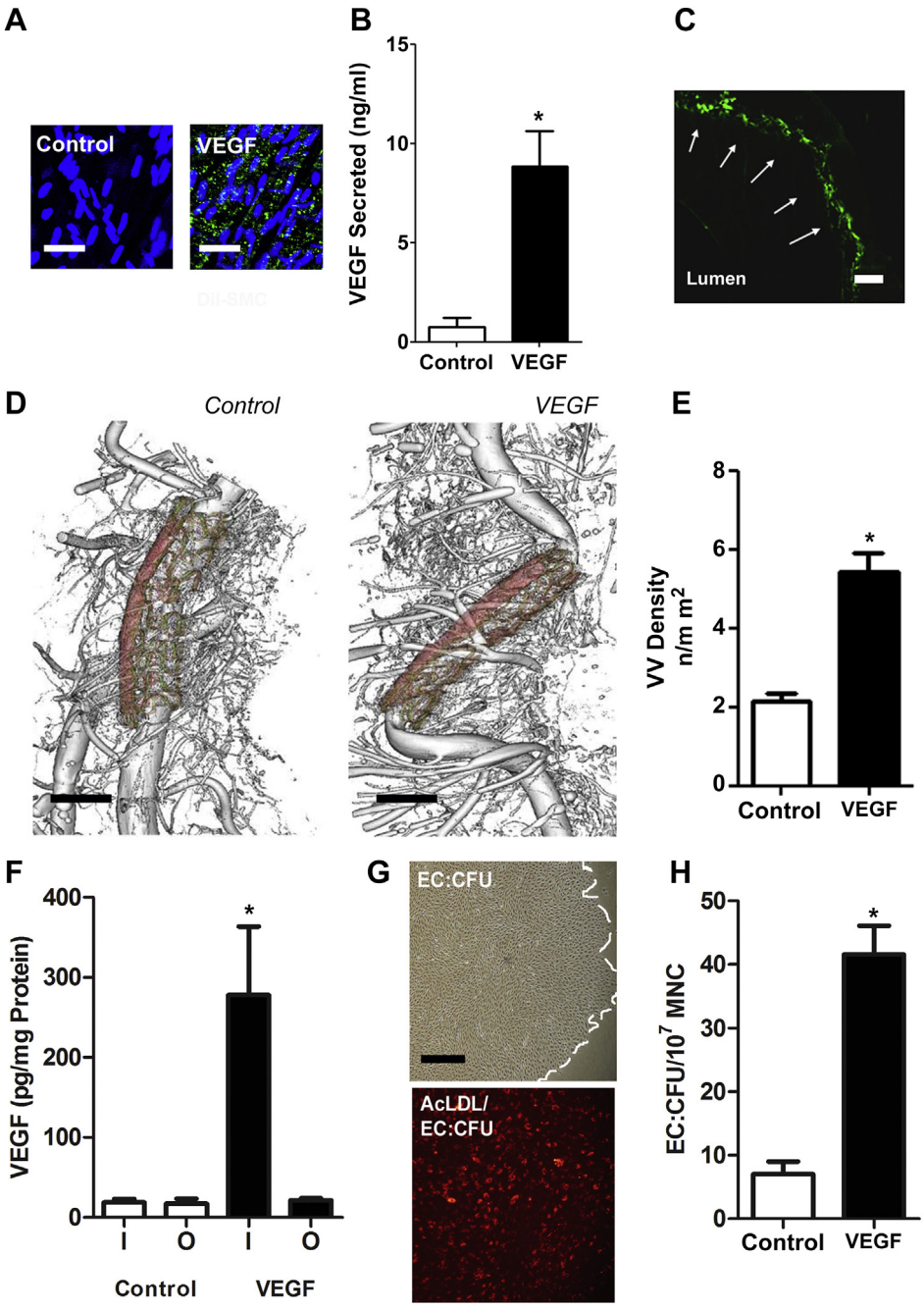

Fig. 2. VEGF-secreting cell mass within ICDD increased angiogenesis and angiogenic indices *in vivo*. **A**. Immunofluorescence analysis of VEGF (green) expression *in vitro* in SMC within ICDD-VEGF with DAPI-stained nuclei (blue) showing a granular localization pattern characteristic of secreted proteins (Scale bar: 50 μm, $n = 3$). **B**. Quantification of VEGF secretion from control or VEGF engineered SMCs by ELISA (*:$p < 0.01$ versus control, $n = 10$). **C**. Transverse section of pig circumflex artery showing stably implanted ICDD with SMC expressing GFP 1 month following implantation (Scale bar: 200 μm). **D,E**. Micro-CT analysis showing increased vasa vasorum density across ICDD recipient segments compared to ICDD-Control treatment of normal coronary arteries (scale bar: 5 mm, *:$p < 0.05$, $n \geq 5$ for each group). **F**. ELISA analysis of ICDD recipient artery and underlying intima (I) or tissue taken from outside the ICDD treated vessel (O) showing increased intimal VEGF levels associated with ICDD-VEGF placement (filled bars) versus control ICDD (open bars) (*:$p < 0.05$, $n \geq 5$ for each group). **G**. Endothelial cell colony forming units (EC:CFU) from the peripheral blood labeled with acetylated LDL (scale bar: 500 μm). **H**. Enhanced EC:CFU in the peripheral blood of pigs treated with ICDD-VEGF versus control. (*:$p < 0.05$, $n \geq 5$ for each group).

assessment (Fig. 6(B)) and regional wall motion by CT (Fig. 6(C and D)) demonstrating significant functional recovery that was concomitant with increased perfusion in the ischemic zone, as well as histologic and immunohistochemical evidence of arteriogenesis.

4. Discussion

Despite decades of advances in pharmacologic, device and surgical treatment of occlusive vascular disease, a cohort of symptomatic, non-revascularizable atherosclerotic patients remain

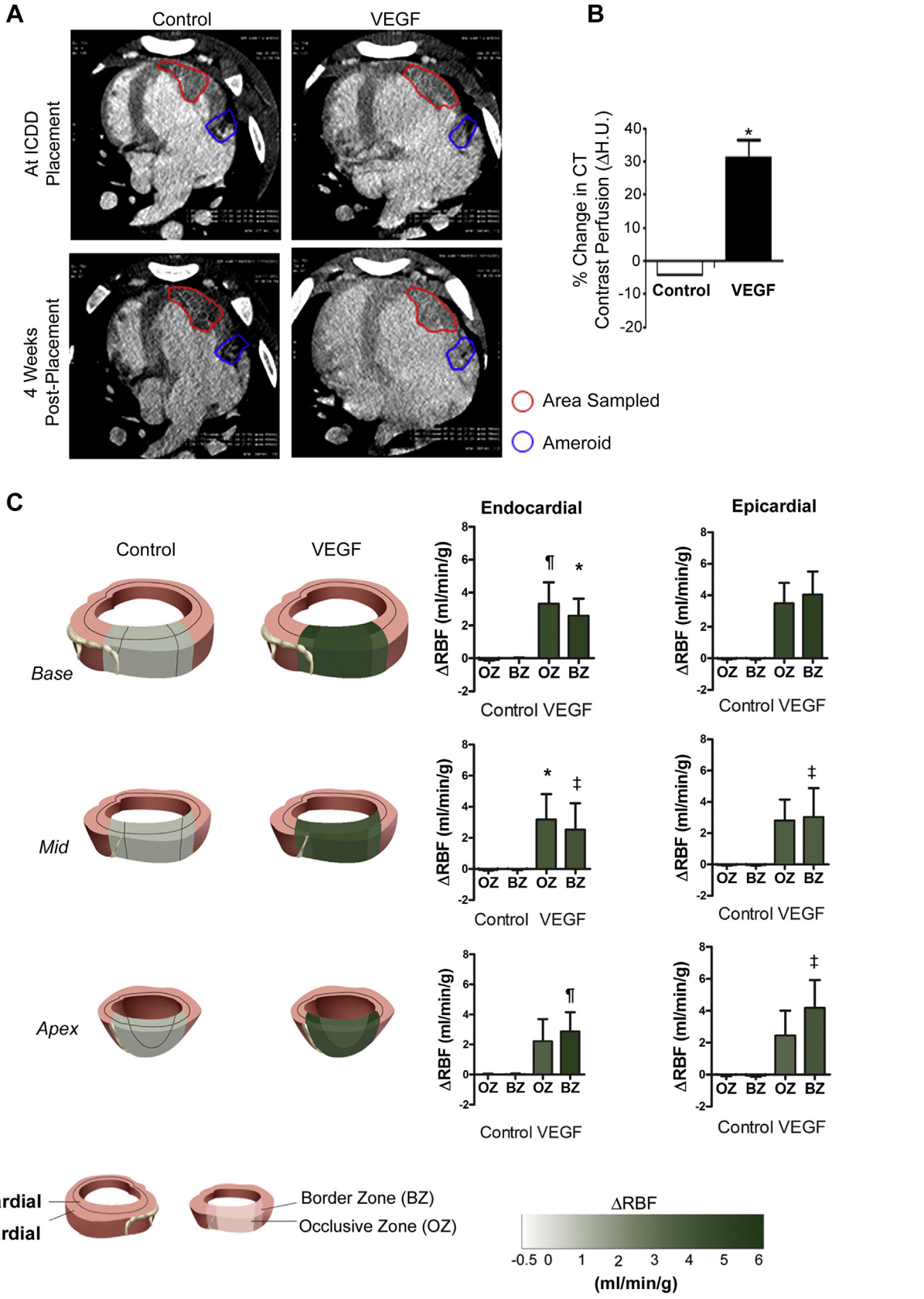

Fig. 3. ICDD-VEGF delivery increased contrast perfusion and regional blood flow at rest in a porcine CTO model. A. Contrast perfusion in ICDD-VEGF and ICDD-Control animals in territory supplied by occluded LCx artery outlined in red at the time of ICDD placement and four weeks later. CT artefact from ameroid constrictor is highlighted (blue). **B**. Quantification of CT contrast perfusion in ICDD-VEGF compared with ICDD-Control expressed as change in Hounsfield units ΔH.U.) between deployment and 4 weeks (*:$p < 0.05$). **C**. Relative changes in MBF following ICDD-Control or ICDD-VEGF placement at rest measured quantitatively by colored microsphere analysis (*: $p < 0.0001$, ¶: $p < 0.001$ ‡: $p < 0.01$; Kruskal Wallis test, $n \geq 6$ per each group). Keys to tissue sampling and color coding representing change in relative blood flow ΔRBF, ml/min/g tissue) between time of ICDD placement and sacrifice is displayed.

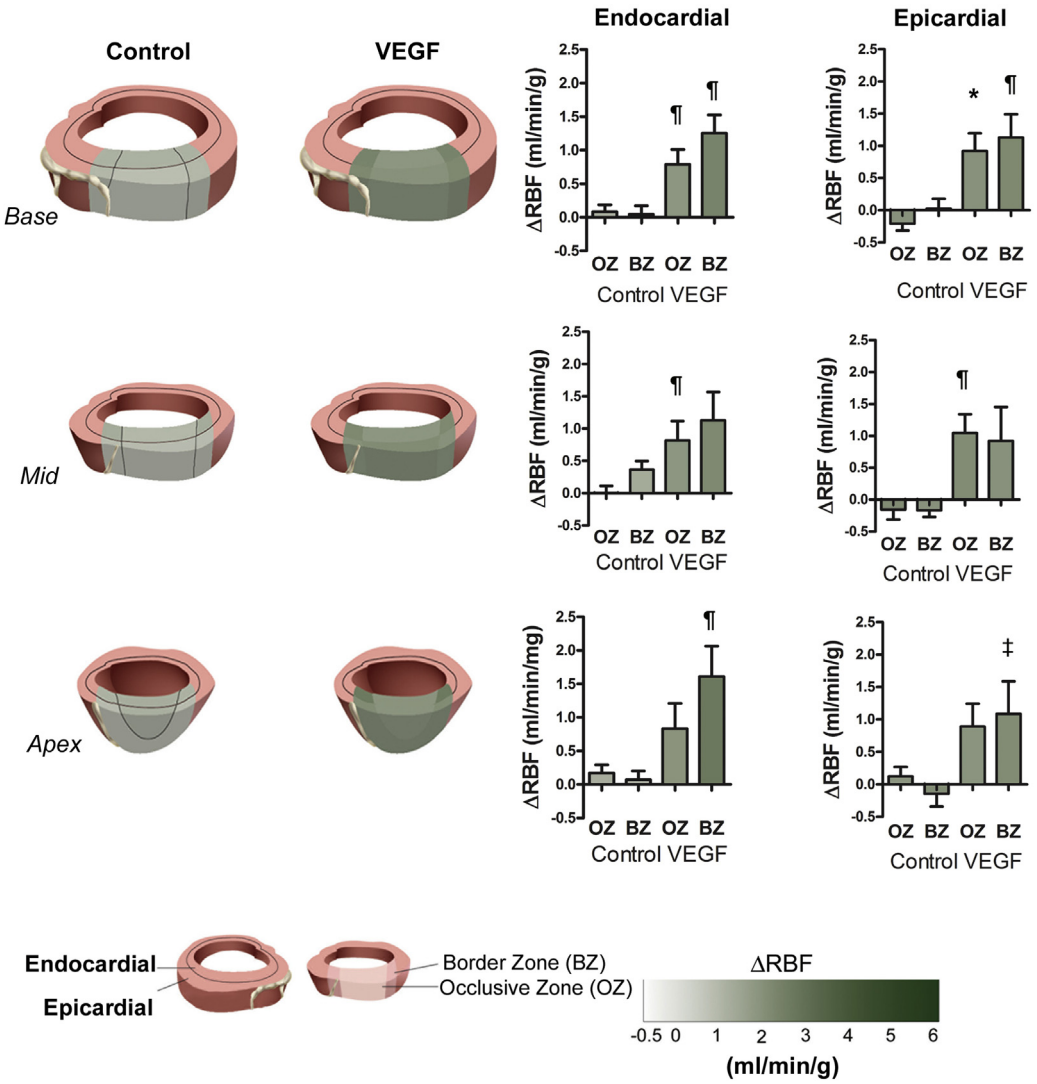

Fig. 4. ICDD-VEGF increased regional blood flow during adenosine cardiac stress in porcine CTO model. Relative changes in MBF four weeks following ICDD-Control or ICDD-VEGF placement during adenosine-induced stress measured quantitatively by colored microsphere analysis (*: $p < 0.0001$, ¶: $p < 0.001$ ‡: $p < 0.01$; Kruskal Wallis test, $n = 10$). Keys to tissue sampling and color coding representing change in relative blood flow ΔRBF, ml/min/g tissue) between time of stent placement and sacrifice is displayed.

[24]. These patients with chronic vascular occlusion are frequently unsuitable for percutaneous coronary intervention (PCI) due to procedural risk and high restenosis rates, and may not be ideal candidates for surgical revascularization due to poor distal vessel targets, unfavorable co-morbidities or lack of suitable bypass conduits [5]. Gene and more recently cell therapy have been touted as a therapeutic answer for these no-option patients [25] but these approaches still lack sufficient site specific targeting, and are hampered by dissipation of therapeutic effect through dilution and dispersion of gene/cell product within the wider vascular system [26].

The aim of this study was to synergize cell and gene therapy benefits using a tissue engineered ICDD to enhance site specific angiogenesis in a model of chronic myocardial ischemia. We posited that an ICDD secreting VEGF transgene product could be delivered safely to a site of chronic vascular occlusion and would promote increased myocardial blood flow and improved cardiac function in the ischemic zone of a porcine ameroid constrictor CTO model. In the current study, we demonstrate that ICDD-VEGF promotes significant increases in regional ischemic zone MBF by gold standard color microsphere detection, regional cardiac function by CT contrast imaging and regional arteriogenesis by immunohistochemical microvessel analysis. Moreover, we show that increased blood flow is likely driven by both vasculogenic and arteriogenic processes incorporating endothelial and SMC-pericyte investment of nascent microvessels. Finally, the functional consequences of this augmented angiogenesis includes $a > 50$ fold increase in ischemic zone MBF in VEGF compared to control-treatment under both rest and adenosine-induced stress conditions, with attendant improvement in regional wall motion and global LV functional parameters.

VEGF has been widely used in the past for stand-alone gene therapy but limitations were observed in terms of plasmid vector dispersion and lack of site specificity when delivered *via* the intravascular delivery route, ineffective therapeutic dosing and lack of transgene persistence in the case of adenoviral vectors

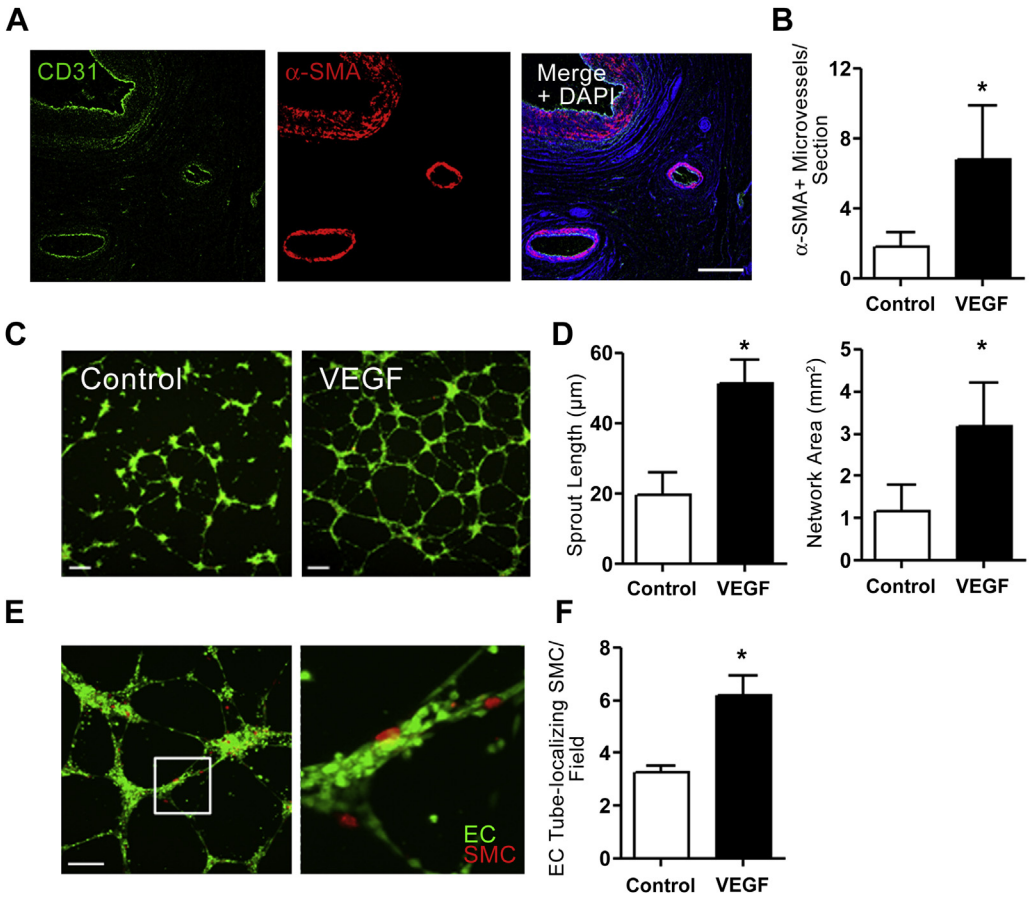

Fig. 5. ICDD-VEGF enhanced angiogenesis *in vivo*, and SMC-VEGF secretome augmented *in vitro* EC tube formation and perivascular SMC association with EC network on matrigel. A. Immunofluorescent analyses of CD31 (green) and α-SMA+ (red) microvessels in myocardial territory supplied by LC*x* (scale bar: 100 μm). **B**. Quantification of microvessel formation showing an increase in α-SMA positive microvessels with ICDD-VEGF placement (*: $p < 0.05$). **C,D** Conditioned media from VEGF-secreting SMC significantly enhanced *in vitro* angiogenic activity of EC cultured in matrigel with regard to sprout length and overall network area (scale bar: 300 μm*: $p < 0.05$). **E**. Conditioned media from VEGF-secreting SMC also increased SMC association with EC tubular networks on matrigel compared to control SMC conditioned media. Note red SMC attached to EC tubes (green tubular network). **F**. Quantification of data represented in **E** ($n \geq 6$ per each group, scale bar: 200 μm, *: $p < 0.05$). (For interpretation of the references to colour in this figure legend, the reader is referred to the web version of this article.)

[26]. ICDD-VEGF gene therapy using autologous SMC stably expressing transgene aimed to address these vector and delivery limitations providing a stable *in vivo* platform for engineered cells that was site specific. The ICDD design allowed precise *ex vivo* calculation of VEGF secretion patterns and dose prior to implantation and facilitated complete protection of cells from barotrauma of balloon deployment and dispersion when compared to more conventional gene delivery strategies [27]. This ICDD approach thus provides a more persistent and stable supply of VEGF locally in addition to the benefit of complementary paracrine factors released from engineered SMC within the device.

Autologous SMCs were selected for high dose stable VEGF gene transfer as well as an ability to facilitate local arteriogenesis not evident in previous single VEGF gene therapy studies [28]. As a substrate for scaffold for cell delivery, the topography of a non-woven and pressed mesh offers many advantages over non-pressed materials including cell coverage, retention and ECM production [29] since the close proximity of the fibers allows cells to proliferate and migrate in a three-dimensional space. The non-woven scaffold geometry was used in combination with fibronectin coating which favors a synthetic phenotype in initially seeded SMC [30] which in turn would enhance cell loading, proliferation within the mesh. We were therefore able to achieve both sustained implanted cell retention and local VEGF production following ICDD placement. SMC were reverted to contractile phenotype with 48 h heparin treatment prior to implantation [31]. We confirmed that conditioned media from VEGF engineered SMC augmented endothelial tube formation and smooth muscle cell pericyte-like association with endothelial tubes on matrigel *in vitro* compared conditioned media from non-engineered SMC (Fig. 5). This supports a complementary paracrine secretome of VEGF engineered SMC that may contribute to additional vasculogenic and arteriogenic components of angiogenesis in our model. Indeed, we show multiple aspects of this angiogenic biology is enhanced by *in vivo* ICDD-VEGF treatment including mobilization of cells with endothelial colony forming potential and α-smooth muscle actin associated microvessel formation (arterioles ≤100 μm in diameter) in the territory supplied by the device. Local VEGF delivery has previously been shown to mobilize and improve survival of circulating [32] and vessel wall [33] derived progenitor cells so it is conceivable that both these effects contributed to angiogenesis in our study. Blood flow to the ICDD-VEGF treated area may allow

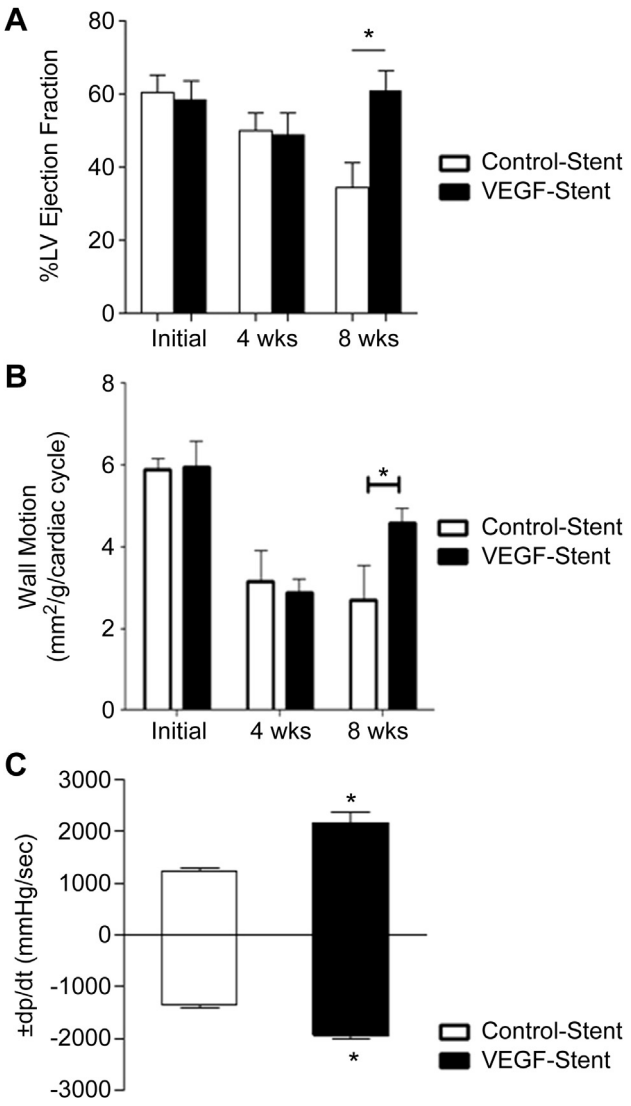

Fig. 6. ICDD-VEGF enhanced global LV ventricular function, hemodynamics and regional wall motion in porcine CTO model. A. Assessment of LV ejection fraction by contrast CT at time of ICDD placement (4 wks) and 1 month later (8 wks) and **B**. d*p*/d*t* by PV loop analysis both showed improvement with ICDD-VEGF compared to ICDD-Control treatment at 8 wks. C. Quantification of the improvement in regional wall motion elicited by ICDD-VEGF delivery compared to ICDD-Control treatment ($n \geq 6$ per each group, *:$p < 0.05$). Initial histogram data in panels A and B relate to baseline CT parameters in pigs before creation of vascular occlusions with ameroid.

circulating cells known to express VEGF receptors including monocytes, and blood-derived progenitor cells, contact with a low level continual source of VEGF. Circulating monocytic cells, whose subpopulations include putative endothelial cell colony forming cells, augmented in our study, may also functionally contribute to this angiogenesis, as previously demonstrated by others in models of peripheral ischemia [34].

We further hypothesize that local production of VEGF creates a concentration gradient which promotes capillary sprouts and that additional secretion of other growth factors by resident smooth muscle cells and perhaps other cells in the local area of the stent contributes to both angiogenesis and arteriogeneisis in the ischemic myocardial region supplied by the ICDD. Secretion of complementary growth factors by resident and VEGF-engineered SMC may also have contributed to arteriogeneisis in the ischemic myocardial region supplied by the ICDD. It is conceivable that this arteriogenic network connects with the microvasculature within the ischemic region beyond the initial site of delivery and that additional secretion of complementary growth factors such as PDGF by engineered SMC [10] may have augmented arteriogenesis in the ICDD-VEGF setting. This is borne out by the marked increases in downstream blood flow observed in our microsphere analysis experiments. Previous evidence from murine intramuscular gene therapy models indicates that elevated VEGF concentrations in a local microenvironment as opposed to a total systemic dose is a key determinant of angiogenesis following vector delivery [35]. Indeed, a “spatial delivery-efficacy mismatch” has been identified in the case of intramyocardial injections of VEGF in which an improvement of MBF is observed at sites adjacent to, in addition to those directly targeted by injections [36]. In our own study this concept is supported by the marked increases in downstream blood flow observed in our microsphere analysis experiments. Such local VEGF concentration gradients contributing to arteriogenesis have also been demonstrated by others in non-cardiac environments [37].

Formation of capillary networks instead of larger conductance microvessels has been identified as one of the shortcomings of earlier therapeutic angiogenesis strategies. Accepting Poisseuille's law on flow relating to the fourth potency of diameter, in order to replace a conductance artery, a large number of capillaries would need to be created. Although we did not specifically test for vessel leakage with dye methodology, the microvessels we observed histologically were of good morphology with both SMC and endothelial cell elements. Our data indicate that new, and stable microvascular networks, formed post ICDD-VEGF treatment, were capable of appropriate exercise load and regional functional augmentation responses approaching those previously achieved by macrovascular bypass [38]. More importantly, we show here that augmented microvascular angiogenesis present in the ICDD-VEGF group can improve global LV function an effect that may have implications for chronic ischemic cardiomyopathy treatment. For instance, a large proportion of cell therapy studies are currently targeted at this specific patient cohort.

Given that the backbone of the ICDD involves a conventional stent design which aids percutaneous delivery we anticipated that SMC seeded within the stent would cause some neointimal response as predicted from previous work [9]. However since our therapeutic angiogenesis strategy involved acceptance of a pre-existing CTO lesion that in this model, would not be macroluminally revascularized or stented we believed that some in-device restenosis would be acceptable during the proof of concept phase of development. It is possible that future iterations of this ICDD platform could incorporate additional elements that might include biodegradability, on-off transgene regulation and restenosis mitigation strategies. Importantly our data confirm that, although some restenosis was observed especially on the distal end of the ICDD (Supplementary Fig. IV), this did not prospectively impair the robust angiogenic capacity of the implanted device. Indeed we know of no other large animal gene therapy study with a similar augmentation in blood flow between control rest-ischemic and ICDD-VEGF stress-ischemic states.

5. Conclusions

This cell-based, percutaneously delivered, gene therapy system presented as a proof of concept study can provide a sustained

therapeutic transgene product that significantly improves blood flow to ischemic myocardium, translating into regional and global left ventricular functional recovery. This system may have implications for non-revascularizable no-option patients or may be adapted to other vascular beds such as in the peripheral circulation.

Funding sources

This work was supported by grants from the National Institute of Health (NIH-HL66958) and Science Foundation Ireland (NMC – 07/RFP/BIMF816, 10/IN.1/B3034). This work was also supported by an equipment grant from the National Biophotonics Imaging Platform within the Programme for Research at Third Level Institutions Cycle (RCSI/NBIP/CEMP11).

Acknowledgments

We wish to thank Sanja Trinki for graphic design, Cindy Reed, and Jill Allen for technical assistance. The authors also wish to thank Mr Cormac O'Brien of the National Centre for Laser Applications (NCLA) at the National University of Ireland, Galway for assistance in ICDD preparation.

Appendix A. Supplementary data

Supplementary data related to this article can be found at http://dx.doi.org/10.1016/j.biomaterials.2014.07.016.

References

[1] Simons M, Annex BH, Laham RJ, Kleiman N, Henry T, Dauerman H, et al. Pharmacological treatment of coronary artery disease with recombinant fibroblast growth factor-2: double-blind, randomized, controlled clinical trial. Circulation 2002;105:788–93.
[2] Prasad A, Rihal CS, Lennon RJ, Wiste HJ, Singh M, Holmes Jr DR. Trends in outcomes after percutaneous coronary intervention for chronic total occlusions: a 25-year experience from the Mayo Clinic. J Am Coll Cardiol 2007;49:1611–8.
[3] Suero JA, Marso SP, Jones PG, Laster SB, Huber KC, Giorgi LV, et al. Procedural outcomes and long-term survival among patients undergoing percutaneous coronary intervention of a chronic total occlusion in native coronary arteries: a 20-year experience. J Am Coll Cardiol 2001;38:409–14.
[4] Roques F, Nashef SA, Michel P, Gauducheau E, de Vincentiis C, Baudet E, et al. Risk factors and outcome in European cardiac surgery: analysis of the EuroSCORE multinational database of 19030 patients. Eur J Cardiothorac Surg 1999;15:816–22. discussion 22–23.
[5] Caplice NM, Gersh BJ, Alegria JR. Cell therapy for cardiovascular disease: what cells, what diseases and for whom? Nat Clin Pract Cardiovasc Med 2005;2:37–43.
[6] Klugherz BD, Meneveau NF, Kolansky DM, Herrmann HC, Schiele F, Matthai Jr WH, et al. Predictors of clinical outcome following percutaneous intervention for in-stent restenosis. Am J Cardiol 2000;85:1427–31.
[7] Carmeliet P. VEGF gene therapy: stimulating angiogenesis or angioma-genesis? Nat Med 2000;6:1102–3.
[8] Von Degenfeld G, Banfi A, Springer ML, Blau HM. Myoblast-mediated gene transfer for therapeutic angiogenesis and arteriogenesis. Br J Pharmacol 2003;140:620–6.
[9] Panetta CJ, Miyauchi K, Berry D, Simari RD, Holmes DR, Schwartz RS, et al. A tissue-engineered stent for cell-based vascular gene transfer. Hum Gene Ther 2002;13:433–41.
[10] Cao R, Brakenhielm E, Pawliuk R, Wariaro D, Post MJ, Wahlberg E, et al. Angiogenic synergism, vascular stability and improvement of hind-limb ischemia by a combination of PDGF-BB and FGF-2. Nat Med 2003;9:604–13.
[11] Ross R. The smooth muscle cell. II. Growth of smooth muscle in culture and formation of elastic fibers. J Cell Biol 1971;50:172–86.
[12] Roth DM, White FC, Mathieu-Costello O, Guth BD, Heusch G, Bloor CM, et al. Effects of left circumflex ameroid constrictor placement on adrenergic innervation of myocardium. Am J Physiol 1987;253:H1425–34.
[13] Kumar AH, McCauley SD, Hynes BG, O'Dea J, Caplice NM. Improved protocol for processing stented porcine coronary arteries for immunostaining. J Mol Histol 2011;42:187–93.
[14] Simper D, Stalboerger PG, Panetta CJ, Wang S, Caplice NM. Smooth muscle progenitor cells in human blood. Circulation 2002;106:1199–204.
[15] Gossl M, Rosol M, Malyar NM, Fitzpatrick LA, Beighley PE, Zamir M, et al. Functional anatomy and hemodynamic characteristics of vasa vasorum in the walls of porcine coronary arteries. Anat Rec A Discov Mol Cell Evol Biol 2003;272:526–37.
[16] Mannheim D, Versari D, Daghini E, Gossl M, Galili O, Chade A, et al. Impaired myocardial perfusion reserve in experimental hypercholesterolemia is independent of myocardial neovascularization. Am J Physiol Heart Circ Physiol 2007;292:H2449–58.
[17] O'Sullivan JF, Leblond AL, O'Dea J, Hristova I, Kumar S, Martin K, et al. Multidetector computed tomography accurately defines infarct size, but not microvascular obstruction after myocardial infarction. J Am Coll Cardiol 2013;61:208–10.
[18] Arnaoutova I, Kleinman HK. In vitro angiogenesis: endothelial cell tube formation on gelled basement membrane extract. Nat Protoc 2010;5:628–35.
[19] Ferrara N. Binding to the extracellular matrix and proteolytic processing: two key mechanisms regulating vascular endothelial growth factor action. Mol Biol Cell 2010;21:687–90.
[20] Langheinrich AC, Michniewicz A, Sedding DG, Walker G, Beighley PE, Rau WS, et al. Correlation of vasa vasorum neovascularization and plaque progression in aortas of apolipoprotein E(-/-)/low-density lipoprotein(-/-) double knockout mice. Arterioscler Thromb Vasc Biol 2006;26:347–52.
[21] Kalka C, Masuda H, Takahashi T, Gordon R, Tepper O, Gravereaux E, et al. Vascular endothelial growth factor(165) gene transfer augments circulating endothelial progenitor cells in human subjects. Circ Res 2000;86:1198–202.
[22] Möhlenkamp S, Beighley PE, Pfeifer EA, Behrenbeck TR, Sheedy PF, Ritman EL. Intramyocardial blood volume, perfusion and transit time in response to embolization of different sized microvessels. Cardiovasc Res 2003;57:843–52.
[23] Choi JH, Chang SA, Choi JO, Song YB, Hahn JY, Choi SH, et al. Frequency of myocardial infarction and its relationship to angiographic collateral flow in territories supplied by chronically occluded coronary arteries. Circulation 2013;127:703–9.
[24] Svorkdal N. Treatment of inoperable coronary disease and refractory angina: spinal stimulators, epidurals, gene therapy, transmyocardial laser, and counterpulsation. Semin Cardiothorac Vasc Anesth 2004;8:43–58.
[25] Losordo DW, Vale PR, Symes JF, Dunnington CH, Esakof DD, Maysky M, et al. Gene therapy for myocardial angiogenesis: initial clinical results with direct myocardial injection of phVEGF165 as sole therapy for myocardial ischemia. Circulation 1998;98:2800–4.
[26] Leiden JM. Human gene therapy: the good, the bad, and the ugly. Circ Res 2000;86:923–5.
[27] Flugelman MY, Virmani R, Leon MB, Bowman RL, Dichek DA. Genetically engineered endothelial cells remain adherent and viable after stent deployment and exposure to flow in vitro. Circ Res 1992;70:348–54.
[28] Le Ricousse-Roussanne S, Barateau V, Contreres JO, Boval B, Kraus-Berthier L, Tobelem G. Ex vivo differentiated endothelial and smooth muscle cells from human cord blood progenitors home to the angiogenic tumor vasculature. Cardiovasc Res 2004;62:176–84.
[29] Turner NJ, Kielty CM, Walker MG, Canfield AE. A novel hyaluronan-based biomaterial (Hyaff-11®) as a scaffold for endothelial cells in tissue engineered vascular grafts. Biomaterials 2004;25:5955–64.
[30] Stegemann JP, Hong H, Nerem RM. Mechanical, biochemical, and extracellular matrix effects on vascular smooth muscle cell phenotype. J Appl Physiol 2005;98:2321–7.
[31] Caplice NM, West MJ, Campbell GR, Campbell J. Inhibition of human vascular smooth muscle cell growth by heparin. Lancet 1994;344:97–8.
[32] Hattori K, Dias S, Heissig B, Hackett NR, Lyden D, Tateno M, et al. Vascular endothelial growth factor and angiopoietin-1 stimulate postnatal hematopoiesis by recruitment of vasculogenic and hematopoietic stem cells. J Exp Med 2001;193:1005–14.
[33] Hu Y, Zhang Z, Torsney E, Afzal AR, Davison F, Metzler B, et al. Abundant progenitor cells in the adventitia contribute to atherosclerosis of vein grafts in ApoE-deficient mice. J Clin Invest 2004;113:1258–65.
[34] Heil M, Ziegelhoeffer T, Pipp F, Kostin S, Martin S, Clauss M, et al. Blood monocyte concentration is critical for enhancement of collateral artery growth. Am J Physiol Heart Circ Physiol 2002;283:H2411–9.
[35] Ozawa CR, Banfi A, Glazer NL, Thurston G, Springer ML, Kraft PE, et al. Microenvironmental VEGF concentration, not total dose, determines a threshold between normal and aberrant angiogenesis. J Clin Invest 2004;113:516–27.

[36] Radke PW, Heinl-Green A, Frass OM, Griesenbach U, Ferrari S, Geddes DM, et al. Effects of intramyocardial pVEGF165 delivery on regional myocardial blood flow: evidence for a spatial 'delivery-efficacy' mismatch. Gene Ther 2004;11:1249–55.

[37] Webber MJ, Tongers J, Newcomb CJ, Marquardt KT, Bauersachs J, Losordo DW, et al. Supramolecular nanostructures that mimic VEGF as a strategy for ischemic tissue repair. Proc Natl Acad Sci U S A 2011;108:13438–43.

[38] Gunning MG, Chua TP, Harrington D, Knight CJ, Burman E, Pennell DJ, et al. Hibernating myocardium: clinical and functional response to revascularisation. Eur J Cardiothorac Surg 1997;11:1105–12.